

## The Extraction of Anisotropic Contributions in Turbulent Flows

Itai Arad<sup>1</sup>, Brindesh Dhruva<sup>2</sup>, Susan Kurien<sup>1,2</sup>, Victor S. L'vov<sup>1,3</sup>, Itamar Procaccia<sup>1</sup> and K.R. Sreenivasan<sup>2</sup>

<sup>1</sup>*Department of Chemical Physics, The Weizmann Institute of Science, Rehovot 76100, Israel*

<sup>2</sup>*Mason Laboratory and the Dept. of Physics, Yale University, New Haven, CT 06520-8286, USA*

<sup>3</sup>*Institute of Automatization and Electrometry Ac. Sci. of Russia, Novosibirsk 630090, Rusia*

We analyze turbulent velocity signals measured by two probes in the atmosphere, both at the height of 35 meters but displaced by 40 cm nominally orthogonal to the mean wind. Choosing a suitable coordinate system with respect to that of the mean wind, we derive theoretical forms for second order structure functions, and fit them to experimental data. We show that the effect of flow anisotropy is small on the longitudinal component but significant on the transverse component. The data provide an estimate of a universal exponent from among a hierarchy that governs the decay of flow anisotropy with the scale-size.

Experimental studies of turbulent flows are usually limited in the sense that one measures the velocity field at a single spatial point as a function of time [1], and uses Taylor's hypothesis to identify velocity increments at different times with those across spatial length scales,  $R$ . The standard outputs of such measurements are the longitudinal two-point differences of the Eulerian velocity field and their moments, termed structure functions:

$$S_n(R) = \left\langle \left| [\mathbf{u}(\mathbf{r} + \mathbf{R}, t) - \mathbf{u}(\mathbf{r}, t)] \cdot \frac{\mathbf{R}}{R} \right|^n \right\rangle, \quad (1)$$

where  $\langle \cdot \rangle$  denotes averaging over time. In isotropic homogeneous turbulence, these structure functions are observed to behave as a power-law in  $R$ ,  $S_n(R) \sim R^{\zeta_n}$ , with apparently universal scaling exponents  $\zeta_n$  [2].

Recent progress in measurements [3] and in simulations [4] begins to offer information about the tensorial nature of structure functions. Ideally, one would like to measure the tensorial  $n$ th order structure functions defined as

$$S_n^{\alpha_1 \dots \alpha_n}(\mathbf{R}) \equiv \langle [u^{\alpha_1}(\mathbf{r} + \mathbf{R}) - u^{\alpha_1}(\mathbf{r})] \times [u^{\alpha_2}(\mathbf{r} + \mathbf{R}) - u^{\alpha_2}(\mathbf{r})] \dots [u^{\alpha_n}(\mathbf{r} + \mathbf{R}) - u^{\alpha_n}(\mathbf{r})] \rangle, \quad (2)$$

where the superscript  $\alpha_i$  indicates the velocity component in the direction  $i$ . Such information should be useful in studying the anisotropic effects induced by all practical means of forcing. In analyzing experimental data the model of "homogeneous, isotropic small-scale" is universally adopted, but it is important to examine the relevance of this model for realistic flows. One of the points of this Letter is that keeping the tensorial information

helps significantly in disentangling different scaling contributions to structure functions [5]. Especially when anisotropy might lead to different scaling exponents for different tensorial components, a careful study of the various contributions is needed. We will show below that atmospheric measurements contain important anisotropic contributions to one type of transverse structure functions.

In this Letter we analyze measurements in atmospheric turbulence at Taylor microscale Reynolds numbers of about 20,000 [6]. The data were acquired simultaneously from two single-wire probes separated by 40 cm nominally orthogonal to the mean wind direction. The two probes were mounted at a height of about 35 m above the ground on a meteorological tower at the Brookhaven National Laboratory. The hot-wires, about 0.7 mm in length and 6  $\mu\text{m}$  in diameter, were calibrated just prior to mounting them on the tower (and checked immediately after dismounting), and operated on DISA 55M01 constant-temperature anemometers. The frequency response of the hot-wires was typically good up to 20 kHz. The voltages from the anemometers were suitably low-pass filtered and digitized. The voltages were constantly monitored on an oscilloscope to ensure that they did not exceed the digitizer limits. Also monitored on-line were spectra from an HP 3561A Dynamic Signal Analyzer. The wind speed and direction were independently monitored by a vane anemometer mounted a few meters away from the tower. The real-time duration of data record was limited by the degree of constancy of the speed and direction of the wind. The Kolmogorov scale was about 0.45. Table 1 lists a few relevant facts the data records listed here (this being part of a much larger set). The various symbols have the following meanings:  $\bar{U}$  = local mean velocity,  $u'$  = root-mean-square velocity,  $\langle \varepsilon \rangle$  = energy dissipation obtained by the assumption of local isotropy and Taylor's hypothesis,  $\eta$  and  $\lambda$  are the Kolmogorov and Taylor length scales, respectively, the micro-scale Reynolds number  $R_\lambda \equiv u' \lambda / \nu$ , and  $f_s$  is the sampling frequency.

As a first step we tested whether the separation between the two probes was indeed orthogonal to the mean wind. To this end we computed the cross-correlation function  $\langle u_1(t + \tau) u_2(t) \rangle$  where subscripts 1 and 2 refer to the two probes. If the separation were precisely

$\bar{U}$ ms $^{-1}$	$u'$ ms $^{-1}$	$10^2 \langle \varepsilon \rangle$ , m $^2$ s $^{-3}$	$\eta$ mm	$\lambda$ cm	$R_\lambda$	$f_s$ , per channel, Hz	# of samples
8.3	2.30	7.8	0.45	13	19,500	5,000	$4 \times 10^7$

TABLE I. Basic information about the data analyzed in this paper.

orthogonal to the mean wind, this quantity should be maximum for  $\tau = 0$ . Instead, we found the maximum at 0.03 sec, implying that the separation was not precisely orthogonal to the mean wind. To correct for this effect, the data from the second probe were time-shifted by 0.03 seconds. This amounts to a change in the actual value of the orthogonal distance, and we computed this effective distance to be  $\Delta \approx 31$  cm. Next we tested the isotropy of the flow for separations of the order of  $\Delta$ . Define the “transverse” structure function across  $\Delta$  as  $S_T(\Delta) \equiv \langle [u_1(\bar{U}t) - u_2(\bar{U}t)]^2 \rangle$  and the “longitudinal” structure function as  $S_L(\Delta) \equiv \langle [u_1(\bar{U}t + \bar{U}t_\Delta) - u_1(\bar{U}t)]^2 \rangle$  where  $t_\Delta = \Delta/\bar{U}$ . If the flow were isotropic we would expect [1]

$$S_T(\Delta) = S_L(\Delta) + \frac{\Delta}{2} \frac{\partial S_L(\Delta)}{\partial \Delta}. \quad (3)$$

In the isotropic state both components scale with the same exponent,  $S_{T,L}(\Delta) \propto \Delta^{\zeta_2}$ , and their ratio is computed from (3) to be  $1 + \zeta_2/2 \approx 1.35$  where  $\zeta_2 \approx 0.69$  (see below). The experimental ratio was found to be 1.86, indicating some 40% anisotropy at this scale [7]; we expect even more anisotropy on larger scales.

To obtain a theoretical form of the structure function tensor we first select a natural coordinate system. An obvious choice is the mean-wind direction  $n$  along the  $\alpha = 3$  axis. A second axis is given by the separation vector  $\Delta$  between the two probes. It turns out that *for this particular geometrical configuration* such a two-dimensional coordinate system is sufficient to describe all the non-zero tensor components. This is to be expected since all measurements of velocity and all separations are contained in the plane  $(n, \Delta)$ . We can envision a more general experimental setup which measures velocity components perpendicular to the ground or in which the probes are separated in the vertical direction. In such a situation, we would need to take into consideration tensor components arising from the existence of a non-trivial third direction orthogonal to the  $(n, \Delta)$  plane. We expect that such experiments will in the future allow us to study the antisymmetric components of the tensor (see below).

To continue, we need to write down the tensor form for the general second order structure function (defined by Eq. (2) for  $n = 2$ ) in terms of irreducible representations of the SO(3) rotation group. This tensor can be written in terms of the representations of the direct product of two three-dimensional Euclidean vector spaces (for the indices  $\alpha, \beta$ ) and the space of continuous functions on

the unit sphere (for the direction of  $\mathbf{R}$ ) [8]. The latter is spanned by the spherical harmonics  $Y_{l,m}$ , and the representations of the product space are indexed by  $j$ , denoting a  $2j+1$  dimensional irreducible representation. Every such representation is associated with a scalar function  $c_j(R)$  which is expected to scale with a universal exponent  $\zeta_2^{(j)}$ ; the latter is an increasing function of  $j$  and  $\zeta_2^{(0)} = \zeta_2$ . Previous theoretical considerations [9] led to the estimates  $\zeta_2^{(1)} \approx 1$ ,  $\zeta_2^{(2)} \approx 4/3$ . We are interested in relatively modest anisotropies, and so focus on the lowest order correction to the isotropic ( $j = 0$ ) contribution. In other words, we write

$$S^{\alpha\beta}(\mathbf{R}) = S_{j=0}^{\alpha\beta}(\mathbf{R}) + S_{j=2}^{\alpha\beta}(\mathbf{R}) + \dots \quad (4)$$

We do not have a  $j = 1$  term since the possible contributions to it vanish either because of parity considerations (the structure function itself is even in  $\mathbf{R}$ ) or by the incompressibility constraint. Now the most general form of the tensor can be written down by inspection. The case  $j = 0$  is well known, and we write it as

$$S_{j=0}^{\alpha\beta}(\mathbf{R}) = c_0(R) \left[ (2 + \zeta_2) \delta^{\alpha\beta} - \zeta_2 \frac{R^\alpha R^\beta}{R^2} \right], \quad (5)$$

where  $c_0(R) = c_0 R^{\zeta_2}$ , and  $c_0$  is a non-universal numerical constant that needs to be fitted to the data. The  $j = 2$  component can be written as

$$S_{j=2}^{\alpha\beta}(\mathbf{R}) = c_2(R) \left[ a \delta^{\alpha\beta} + b \frac{R^\alpha R^\beta}{R^2} + d \frac{\delta^{\alpha\beta} (\mathbf{n} \cdot \mathbf{R})^2}{R^2} + e \frac{R^\alpha R^\beta (\mathbf{n} \cdot \mathbf{R})^2}{R^4} + f n^\alpha n^\beta + \frac{g(\mathbf{n} \cdot \mathbf{R})}{2R^2} (R^\alpha n^\beta + R^\beta n^\alpha) \right] \quad (6)$$

where  $c_2(R) = R^{\zeta_2^{(2)}}$ . Here  $a, b, d, e, f$  and  $g$  are unknown coefficients which are independent of  $R$ . This form can be further reduced by imposing the conditions of incompressibility and orthogonality with the  $j = 0$  part of the tensor. This leaves us with only two independent coefficients of the form

$$S_{j=2}^{\alpha\beta}(\mathbf{R}) = a R^{\zeta_2^{(2)}} \left[ (\zeta_2^{(2)} - 2) \delta^{\alpha\beta} - \zeta_2^{(2)} (\zeta_2^{(2)} + 6) \times \delta^{\alpha\beta} \frac{(\mathbf{n} \cdot \mathbf{R})^2}{R^2} + 2\zeta_2^{(2)} (\zeta_2^{(2)} - 2) \frac{R^\alpha R^\beta (\mathbf{n} \cdot \mathbf{R})^2}{R^4} + ([\zeta_2^{(2)}]^2 + 3\zeta_2^{(2)} + 6) n^\alpha n^\beta - \frac{\zeta_2^{(2)} (\zeta_2^{(2)} - 2)}{R^2} (R^\alpha n^\beta + R^\beta n^\alpha) (\mathbf{n} \cdot \mathbf{R}) \right] + b R^{\zeta_2^{(2)}} \left[ -(\zeta_2^{(2)} + 3)(\zeta_2^{(2)} + 2) \delta^{\alpha\beta} (\mathbf{n} \cdot \mathbf{R})^2 + \frac{R^\alpha R^\beta}{R^2} + (\zeta_2^{(2)} + 3)(\zeta_2^{(2)} + 2) n^\alpha n^\beta + (2\zeta_2^{(2)} + 1)(\zeta_2^{(2)} - 2) \times \frac{R^\alpha R^\beta (\mathbf{n} \cdot \mathbf{R})^2}{R^4} - ([\zeta_2^{(2)}]^2 - 4) (R^\alpha n^\beta + R^\beta n^\alpha) (\mathbf{n} \cdot \mathbf{R}) \right]. \quad (7)$$

Finally, we note that in the present experimental set-up only the component of the velocity in the direction of  $\mathbf{n}$

$\zeta_2$	$\zeta_2^{(2)}$	$c_0$	$a$	$b$
0.69	1.36	0.112	-0.052	0.050

TABLE II. The scaling exponents and the three coefficients in units of  $(\text{m/sec})^2$  as determined from the nonlinear fit of Eqs. (9) to the data.

is measured. In the coordinate system chosen above we can read from (7) the relevant component as

$$\begin{aligned}
 S^{33}(R, \theta) &= S_{j=0}^{33}(R, \theta) + S_{j=2}^{33}(R, \theta) \quad (8) \\
 &= c_0 \left( \frac{R}{\Delta} \right)^{\zeta_2} \left[ 2 + \zeta_2 - \zeta_2 \cos^2 \theta \right] \\
 &\quad + a \left( \frac{R}{\Delta} \right)^{\zeta_2^{(2)}} \left[ (\zeta_2^{(2)} + 2)^2 - \zeta_2^{(2)}(3\zeta_2^{(2)} + 2) \cos^2 \theta \right. \\
 &\quad \left. + 2\zeta_2^{(2)}(\zeta_2^{(2)} - 2) \cos^4 \theta \right] \\
 &\quad + b \left( \frac{R}{\Delta} \right)^{\zeta_2^{(2)}} \left[ (\zeta_2^{(2)} + 2)(\zeta_2^{(2)} + 3) - \zeta_2^{(2)}(3\zeta_2^{(2)} + 4) \cos^2 \theta \right. \\
 &\quad \left. + (2\zeta_2^{(2)} + 1)(\zeta_2^{(2)} - 2) \cos^4 \theta \right].
 \end{aligned}$$

Here  $\theta$  is the angle between  $\mathbf{R}$  and  $\mathbf{n}$ , and we normalized  $R$  by  $\Delta$  making all our coefficients dimensional, with units of  $(\text{m/sec})^2$ .

To fit our experimental results we converted, using Taylor's hypothesis, the structure functions computed from time differences for a single probe, and cross differences between the two probes, to components of the form (8) with  $\theta = 0$  and with variable  $\theta$ , respectively. In other words,

$$S^{33}(R, \theta = 0) = \langle [u_1(\bar{U}t + \bar{U}t_R) - u_1(\bar{U}t)]^2 \rangle, \quad (9)$$

where  $t_R \equiv R/\bar{U}$ , and

$$S^{33}(R, \theta) = \langle [u_1(\bar{U}t + \bar{U}t_{\tilde{R}}) - u_2(\bar{U}t)]^2 \rangle \quad (10)$$

Here  $\theta = \arctan(\Delta/\bar{U}t_{\tilde{R}})$ ,  $t_{\tilde{R}} = \tilde{R}/\bar{U}$ , and  $R = \sqrt{\Delta^2 + (\bar{U}t_{\tilde{R}})^2}$ . We then found the three unknown coefficients  $c_0$ ,  $a$  and  $b$ , and the two exponents  $\zeta_2$  and  $\zeta_2^{(2)}$  by a nonlinear fit to the form (8). The fitted numbers are presented in Table 2.

One surprise of the analysis is that the  $\theta = 0$  (purely longitudinal) structure function is hardly affected by the anisotropy. The reason is the very close numerical absolute values of the coefficients  $a$  and  $b$ . In the case  $\theta = 0$  the two tensor forms multiplied by  $a$  and  $b$  coincide, and the  $j = 2$  contribution becomes very small. We believe that this is the main reason that the effect of anisotropy has been disregarded by and large in atmospheric experiments. The component  $S^{33}(R, \theta = 0)$  can be reasonably fitted by a power law with single exponent. In fact, the value of  $\zeta_2 = 0.69$  quoted above can be obtained from

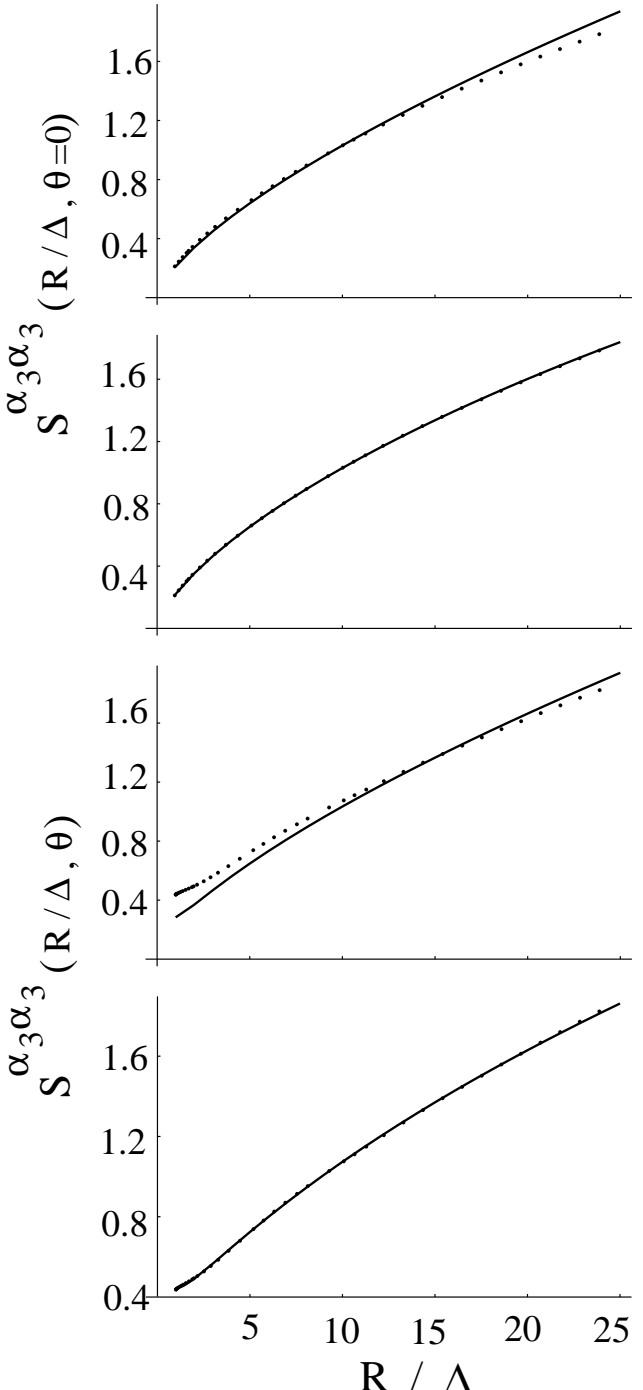


FIG. 1. The structure functions  $S^{33}$  for  $\theta = 0$  in panels (a) and (b), and for non-zero  $\theta$  in panels (c) and (d). The dots are for experimental data and the line is the analytic fit. Panels (a) and (c) present fits to the  $j = 0$  component only, and panels (b) and (d) to components  $j = 0$  and  $j = 2$  together.

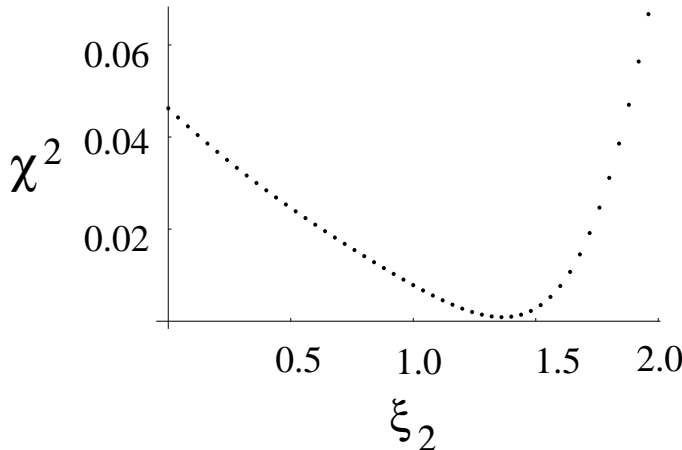


FIG. 2. The determination of the exponent  $\zeta_2^{(2)}$  from a least-square fit of  $S^{33}(R, \theta)$  to its analytic form. The numerical value of the best fit,  $\xi = 1.36 \pm 0.1$  is in close agreement with the theoretical expectation of  $4/3$  (without intermittency corrections).

such a simple fit, and as long as one measures only this component, there is no reason for a more sophisticated analysis. In fact,  $\zeta_2$  is so well estimated that we can safely take it as fixed when we perform the simultaneous fit of all the other unknowns.

On the other hand, the finite  $\theta$  components are strongly affected by the anisotropy, and the inclusion of the second exponent  $\zeta_2^{(2)}$  is essential for a good fit. In Fig. 1 we exhibit various quantities as a function of  $R/\Delta$ ; the first panel shows  $S^{33}(R, \theta = 0)$  with its best fit to the  $j = 0$  contributions, and in panel (b) with its best fit to the sum of  $j = 0$  and  $j = 2$ . The differences, though small as noted previously, are enough to produce an improved agreement. Similarly in panels (c) and (d) we show  $S^{33}(R, \theta)$  with its best fit to the  $j = 0$  and the sum of  $j = 0$  and  $j = 2$ , respectively. It is clear that panel (c) does not give an adequate fit in the “inertial range”, as estimated from panel (a) to range up to, say,  $15\Delta$ . If we tried to read a log-log slope from the data in panel (c) we would get an apparent scaling exponent  $\zeta_2$  considerably smaller than  $0.69$ . The excellent fits in panels (b) and (d) are a good support to the present mode of analysis.

To our knowledge, this determination of  $\zeta_2^{(2)}$  is the first instance of finding an exponent describing the degree of anisotropy. The close agreement with the theoretical expectation of  $4/3$  (e.g., Ref. [10]) is a strong indication that this exponent is universal. In Fig. 2 we present  $\chi^2$  (the sum of the squares of the differences between the experimental data and the fitted values) as a function of  $\zeta_2^{(2)}$ . The optimal value of this exponent and the uncertainty determined from this plot is  $\zeta_2^{(2)} \approx 1.36 \pm 0.1$ .

It should be understood that the exponent  $\zeta_2^{(2)}$  (and also  $\zeta_2^{(1)}$  that is unavailable from the present measure-

ments) are just the smallest exponents in the hierarchy  $\zeta_2^{(j)}$  that characterizes higher order irreducible representations indexed by  $j$ . The study of these exponents is in its infancy, and considerable experimental and theoretical effort is needed to reach firm conclusions regarding their universality and numerical values. We expect the exponents to be a non-decreasing function of  $j$ , explaining why the highest values of  $j$  are being peeled off quickly when  $R$  decreases. Nevertheless, the lower order values of  $\zeta_2^{(j)}$  can be measured and computed. It is the program of the present authors to proceed in this direction.

At Weizmann, the work was supported by the Basic Research Fund administered by the Israeli Academy of Sciences, the US-Israel Binational Science Foundation and the Naftali and Anna Backenroth-Bronicki Fund for Research in Chaos and Complexity. At Yale, it was supported by the National Science Foundation grant DMR-95-29609, and the Yale-Weizmann Exchange Program.

---

- [1] A.S. Monin and A.M. Yaglom, *Statistical Fluid Mechanics: volume 2* (MIT, Cambridge, 1971).
- [2] U. Frisch, *Turbulence: The Legacy of A.N. Kolmogorov* (Cambridge University Press, Cambridge, 1995); N. Cao, S. Chen and Z.-S. She, Phys. Rev. Lett., **76**, 3711 (1996).
- [3] R. Camussi, D. Barbagallo, G. Guj and F. Stella, Phys. Fluids, **8**, 1181 (1996); A. Noullez, G. Wallace, W. Lempert, R. B. Miles and U. Frisch, J. Fluid Mech. **339**, 287 (1997); B. Dhruba, Y. Tusji and K.R. Sreenivasan, Phys. Rev. E, **56**, R4928 (1997).
- [4] O.M. Boratav, Phys. Fluids, **339**, 287 (1997); S. Chen, K.R. Sreenivasan, M. Nelkin and N. Cao, Phys. Rev. Lett., **79**, 2253 (1997).
- [5] V.S. L'vov, E. Podivilov and I. Procaccia, Phys. Rev. Lett., **79**, 2050 (1997).
- [6] K.R. Sreenivasan and B. Dhruba, Japan Phys. Soc. (to appear)
- [7] In Eq. (3),  $S_T(\Delta)$  is obtained for true spatial separation while  $S_L(\Delta)$  is obtained from Taylor's hypothesis assuming that the proper convection velocity is  $\bar{U}$ . Estimates of convection velocity in boundary layers (e.g., P.A. Krogstad, J.H. Kaspersen and S. Rimestad, Phys. Fluids, **10**, 949 (1998)) show that this might not be precise. Further, the choice of  $\frac{2}{3}\bar{U}$  as the convection speed yields  $S_T(\Delta)/S_L(\Delta) \approx 4/3$ , as required by isotropy. A full assessment of these observations is pending.
- [8] I. Arad, V.S. L'vov and I. Procaccia, Phys. Rev. E., to be published.
- [9] D. C. Leslie, *Developments in the theory of turbulence*. Clarendon Press, Oxford (1973); S. Grossmann, D. Lohse, V. L'vov and I. Procaccia, Phys. Rev. Lett. **73**, 432 (1994); E.A. Kuznetsov and V.S. L'vov, Physica D **2**, 203 (1981).
- [10] J.L. Lumley, Phys. Fluids, **10**, 855 (1967).